XIX IMEKO World Congress
Fundamental and Applied Metrology
September 6–11, 2009, Lisbon, Portugal

CHARACTERISTICS OF CONTROLLED-CLEARANCE PISTON-CYLINDERS FOR PRESSURE RANGES UP TO 1 GPA

Hiroaki Kajikawa, *Kazunori Ide, and Tokihiko Kobata*

National Metrology Institute of Japan (NMIJ), AIST, Tsukuba, Ibaraki, Japan
email: kajikawa.hiroaki@aist.go.jp

Abstract − A new controlled-clearance pressure balance has been developed to improve the hydraulic pressure standard for pressures up to 1 GPa. For several controlled-clearance piston-cylinders, characterization experiments based on the Heydemann-Welch model were performed to estimate the effective area of them. The results for the piston-cylinders of different pressure ranges are exemplified in this paper. Some of the piston-cylinders showed different characteristics from those expected by the model at higher pressures. To change the deformational characteristics in response of the jacket pressure, the area and position of the cylinder on which the jacket pressure is applied was changed by the change in the length of the sleeve in the housing. The 500 MPa piston-cylinder with shorter sleeve showed better linearity in the relationships between the jacket pressure and the cubic root of the piston fall-rate, resulting in the estimation of the zero clearance jacket pressure with smaller error.

Keywords: pressure balance, controlled-clearance piston-cylinder, Heydemann-Welch model

1. INTRODUCTION

National Metrology Institute of Japan (NMIJ, AIST) has established the hydraulic pressure standard in the pressure range up to 1 GPa using several pressure balances and a precise pressure multiplier. When we establish the pressure standard using pressure balances, the main thing in high pressure range is to precisely evaluate the pressure dependence of the effective area of the piston-cylinder because both the piston and cylinder are largely distorted by the pressure. Among several types of piston-cylinder, a controlled-clearance (CC) piston-cylinder has an advantage that pressure distortion of the piston-cylinder is able to be partially controlled. Moreover, the pressure dependence of the effective area is determined independently by characterization experiments. Thus, it is widely used as the primary pressure standard.

A new pressure balance equipped with the CC piston-cylinder is developed at NMIJ with the aim of improving hydraulic pressure standard. At present, there are several CC piston-cylinders of four different pressure ranges: 100 MPa, 200 MPa, 500 MPa, and 1 GPa. Characterization experiments for determining the pressure dependence of the effective area are now in progress.

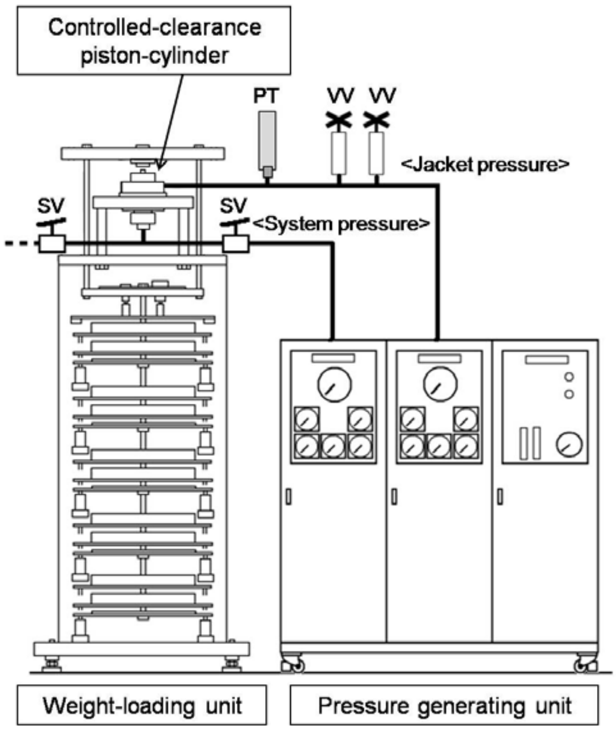

Fig. 1. Schematic viewing of the new controlled-clearance pressure balance. The constituent devices are displayed in different scales for an easy overview. The system pressure line is connected to another pressure balance. PT: pressure transducer, VV: variable volume, SV: shut-off valve.

In this paper, the main features of the controlled-clearance pressure balance in NMIJ are briefly introduced in section 2. The principle and the procedures of the characterization experiments for the CC piston-cylinders based on the Heydemann-Welch model are explained in section 3. Then, the results of the characterization experiments for the CC piston-cylinders of different pressure ranges are shown in section 4. In section 5, the effects of the sleeve length in the housing on the deformational characteristics are discussed. Finally, a brief conclusion is given in section 6.

ISBN 978-963-88410-0-1

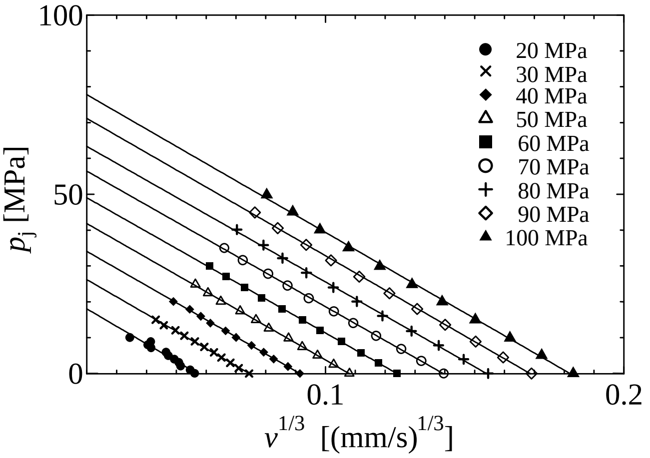

Fig. 2. Piston fall-rate in response to the applied jacket pressure for 100 MPa CC piston-cylinder. p_j is plotted against the cubic root of v. Data at the same p_s is denoted by the same symbols.

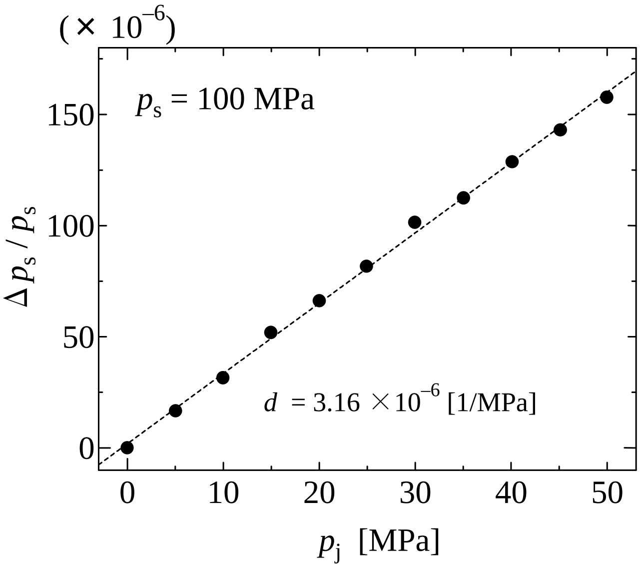

Fig. 3. Relative change in the system pressure, $\Delta p_s/p_s$, against the applied jacket pressure, p_j, at p_s = 100 MPa. Dotted line denotes a linear fitting to the data. The slope of this straight line yields d.

2. APPARATUS

The schematic drawing of the new CC pressure balance is shown in Fig.1. To use the CC pressure balance effectively, two independent pressure sources, the system and jacket pressures, are required. In the pressure generating unit, an oil-operated compressor is used in common, and an intensifier with a nominal ratio of 1:50 is used for each line; the maximum pressure that can be achieved is 1 GPa. To perform cross-float measurements in the characterization experiment, the system pressure line is connected to another pressure balance of free-deformation (FD) type. The jacket pressure is finely adjusted by variable volumes and measured by a pressure transducer.

The weight-loading unit is a suspension type and consists of disk weights of 19 kg and 95 kg, and cylindrical weights of 0,5 kg and 2,5 kg; the total mass of these weights is approximately 1100 kg. Each weight is supported by pneumatic actuators and is able to be lifted up/down independently. Using these mass-loading actuators and digital mass comparators, we calibrated the masses of the weights twice, in 2003 and 2006 [1]. The relative change in the masses between the two calibrations was less than 2 ppm (parts per million) and was well within the uncertainties of the calibrations. From these results, it is confirmed that the weight set has been maintained under suitable conditions and the masses of them are precisely kept.

3. PRINCIPLE AND PROCEDURE OF THE CHARACTERIZATION EXPERIMENTS

To estimate the pressure dependence of the effective area, we start with the Heydemann-Welch (H-W) model [2]. In the model, the effective area is expressed as a function of system pressure, p_s, jacket pressure, p_j, and temperature, T, as:

$$A_e(p_s, p_j, T) = A_{p,T_0} \cdot \{1 + \alpha \cdot (T - T_0)\} \cdot (1 + b_p \cdot p_s) \cdot \{1 + d \cdot (p_z - p_j)\} \quad (1)$$

A_{p,T_0} is the piston area under the standard condition. The reference temperature, T_0, is set to be 23 ^{o}C. α is sum of the thermal expansion coefficients of a piston and cylinder. b_p is the pressure distortion coefficient of a piston. It is calculated from the elastic theory as $b_p = (3\mu - 1) / E$, where μ is Poisson's constant and E is the modulus of elasticity. The forth term of the right-hand side of (1) represents the effect of jacket pressure. Two parameters are introduced: the jacket pressure coefficient, d, and the zero clearance jacket pressure, p_z. These two parameters depend on p_s and are determined by the characterization experiments.

The jacket pressure coefficient shows the relative change in the effective area in response to the jacket pressure, and deduced by,

$$d = \frac{1}{\Delta p_j} \cdot \left(\frac{\Delta p_s}{p_s} \right) . \quad (2)$$

$\Delta p_s/p_s$ is the relative change in the generated pressure and determined by the cross-float measurements against a FD piston-cylinder. In each condition of p_s and p_j, the pressure generated by CC piston-cylinder is equilibrated with that by FD piston-cylinder. Then, $\Delta p_s/p_s$ is actually approximated by the relative change in the mass loaded on the FD piston.

The zero clearance jacket pressure means the hypothetical value of the jacket pressure with which the clearance between the piston and cylinder is assumed to become zero. It is estimated from the change in the piston fall-rate, v, by the application of the jacket pressure, as the equation below:

$$p_j = \frac{1}{K} \cdot v^{1/3} + p_z , \quad (3)$$

where K is a proportional constant. In the experiment, when p_j is plotted against v, p_z is obtained as the y-intercept of the linearly fitted line.

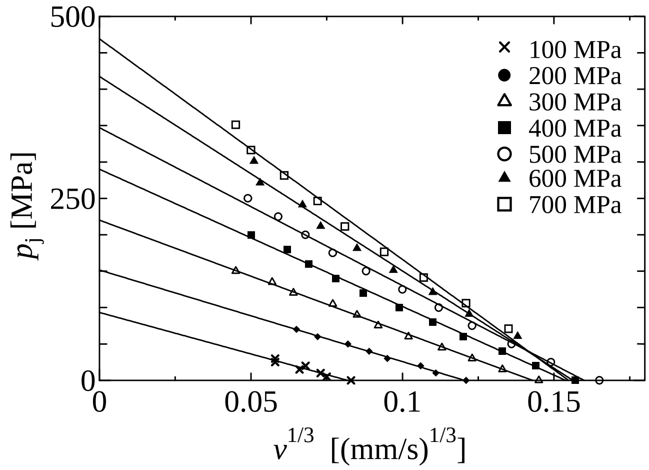

Fig. 4. Piston fall-rate in response to the applied jacket pressure for 1 GPa CC piston-cylinder. p_j is plotted against the cubic root of v. Data at the similar p_s is denoted by the similar symbols.

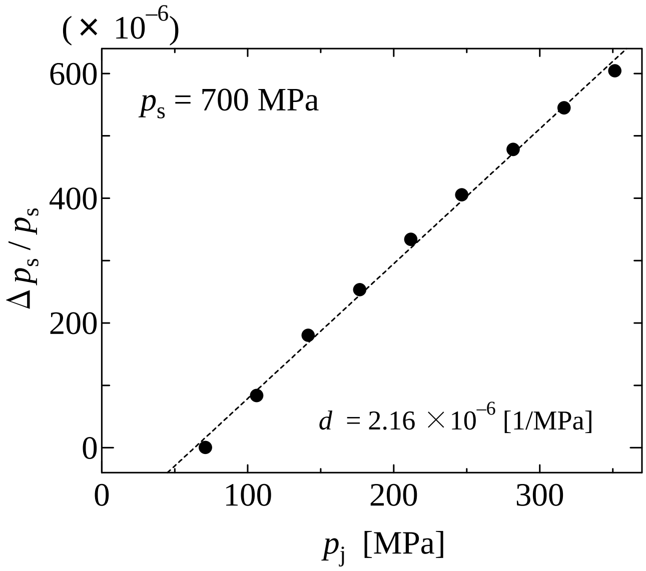

Fig. 5. Relative change in the system pressure, $\Delta p_s/p_s$, against the applied jacket pressure, p_j, at p_s = 700 MPa for the 1 GPa CC piston-cylinder. The pressure at p_j = 70 MPa is taken to be zero. Dotted line denotes a linear fitting to the data.

At present, we have several CC piston-cylinders of different pressure ranges; 100 MPa, 200 MPa, 500 MPa and 1 GPa. Generally, the characterization experiments for determining these two parameters were performed at p_s from 20 % to 100 % of the maximum pressure in steps of 10 % of the maximum pressure. For each p_s, the maximum value of p_j was carefully determined depending on the characteristics of each CC piston-cylinder to avoid excessive application of p_j, which may damage the piston and cylinder. In general, p_j was changed from 0 % to 50 % of p_s in steps of 5 % of p_s. In each condition of p_s and p_j, the cross-float and piston fall-rate measurements were performed after the pressure is stabilized. The waiting time for the pressure stabilization differs from the pressure ranges.

4. RESULTS OF THE CHARACTERIZATION EXPERIMENTS

4.1. Results for the 100 MPa piston-cylinder

The parameters in the H-W model for the 100 MPa CC piston-cylinder were evaluated from the characterization experiments [3]. Results of the experiments are shown in Fig. 2 and Fig. 3. Fig. 2 demonstrates the change in the piston fall-rate in response to p_j. According to (3) in the H-W model, p_j is plotted against $v^{1/3}$. As expected in the model, the data at the same p_s stand in a straight line. Solid line is a linearly fitted line at each p_s. The fitted lines are aligned almost in parallel. p_z is obtained as the y-intercept of the fitted line.

Fig. 3 exemplifies the relative change in the system pressure, $\Delta p_s/p_s$, in response to the applied p_j at p_s = 100 MPa. The generated system pressure without applying p_j is taken as zero. $\Delta p_s/p_s$ increases almost linearly with p_j. Then, d is obtained as the slope of the fitted straight line. In this case, d becomes $3{,}16 \times 10^{-6}$ MPa^{-1}.

Using the resultant $p_z(p_s)$ and $d(p_s)$, we estimated the pressure dependence of the effective area based on (1). After that, to verify our estimation, a FD piston-cylinder for 100 MPa range was calibrated against the evaluated CC piston-cylinder. Then the pressure distortion coefficient, λ, was compared with that calibrated against our present pressure scale. From the calibration against our current pressure scale, λ of the FD piston-cylinder has been determined as $1{,}05 \times 10^{-6}$ ($\pm 1{,}02 \times 10^{-7}$) MPa^{-1}. On the other hand, the value of λ from the calibration against the evaluated CC piston-cylinder became $1{,}06 \times 10^{-6}$ MPa^{-1}. Two results of λ were in good agreement with each other. This comparison indicates that for the 100 MPa CC piston-cylinder, the estimation of the pressure dependence of the effective area based on the H-W model is consistent with that from our current pressure scale.

It is worth noting that the results for the 200 MPa CC piston-cylinder showed the similar characteristics as those for the 100 MPa piston-cylinder.

4.2. Results for the 1 GPa piston-cylinder

Results of the characterization experiments for the 1 GPa piston-cylinder are shown in Fig. 4 and Fig. 5. The results at p_s from 100 MPa to 700 MPa are shown in the figures. p_j was changed according to its characteristics at each p_s. At p_s of 600 MPa and 700 MPa, p_j was changed from 10 % to 50 % of p_s to avoid breaking due to the excessive expansion of the cylinder. Fig. 4 shows the change in the piston fall-rate in response to p_j. Solid line in the figure denotes the linearly fitted line at each p_s. In this case, the data at pressures lower than 400 MPa show a linear relationship, as seen for the 100 MPa piston-cylinder in Fig. 2. However, at higher pressures, a relatively large deviation from the linear relationship was seen over the wide range of p_j. The degree of curvature becomes larger at higher p_s. The slope of the fitted line becomes steeper with increasing p_s; the fitted lines at pressures of 500 MPa and above intersect with each other.

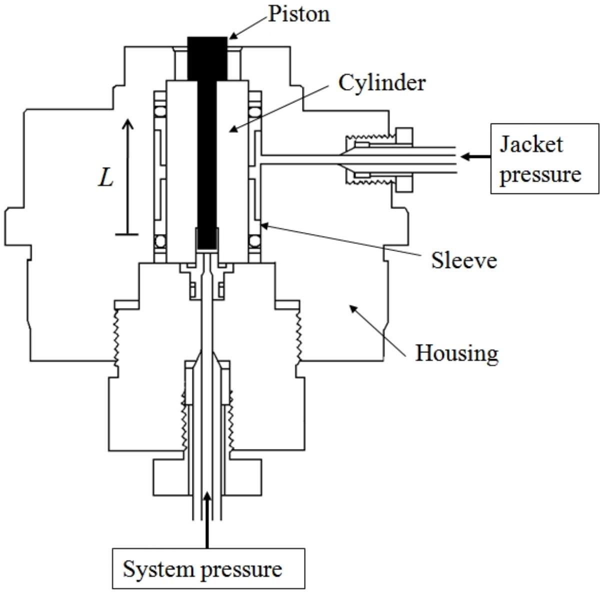

Fig. 6. Schematic Drawing of the controlled-clearance piston-cylinder and a housing. L is the length of the sleeve built into the space for applying the jacket pressure.

Fig. 5 is a plot of $\Delta p_s/p_s$, against p_j at p_s = 700 MPa. The generated pressure with the applied p_j of 70 MPa was taken as zero. Dotted line is a linear fitting to the data. Compared to the result for the 100 MPa piston-cylinder in Fig. 3, in which $\Delta p_s/p_s$ increases almost linearly with p_j, the increasing rate of $\Delta p_s/p_s$ becomes smaller with increasing p_j. That means d decreases with p_j at p_s =700 MPa. It is contradictory to the conventional interpretation in the H-W model that d depends only on p_s. The p_j dependence of d is observed at other system pressures.

Results for a 500 MPa CC piston-cylinder show the similar characteristics as those for the 1 GPa piston-cylinder especially at high system pressures. The results for the 500 MPa piston-cylinder are exemplified in [4].

5. EFFECT OF THE SLEEVE LENGTH ON THE DEFORMATIONAL CHARACTERISTICS

As shown in shown in Fig. 4 and Fig. 5, results of the characterization experiments at higher pressures more than a several hundred MPa showed different behaviour from that expected in the H-W model.

Regarding the piston fall-rate, the linear relationship between $v^{1/3}$ and applied p_j is expected based on the assumptions that the clearance between the piston and cylinder is parallel and that the pressure medium through the clearance flows in the laminar-flow condition [2]. In reality, however, in the condition that the system pressure higher than several hundred MPa is applied to the piston and cylinder and only small jacket pressure is applied on the cylinder from the outside, the lower part of the cylinder is largely expanded by the pressure, then, the clearance of lower part becomes much larger than that of the higher part. Some numerical works using a finite element analysis show

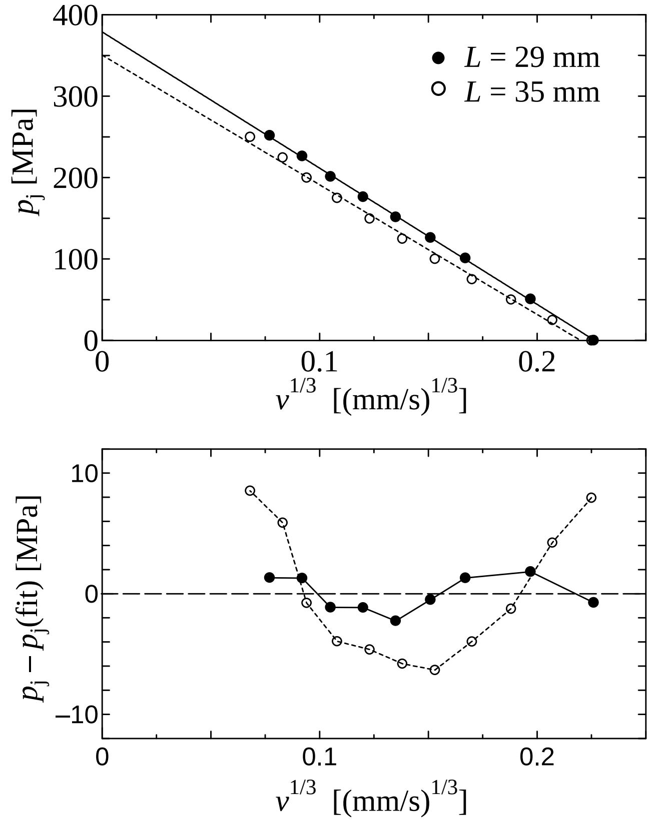

Fig. 7. Piston fall-rate in response to the applied jacket pressure for a 500 MPa CC piston-cylinder with different sleeve length, L; ○ for L = 35 mm and ●for L = 29 mm. (a) Plot of p_j against the cubic root of v. Lines are the linearly fitted lines to the data. (b) Difference between the original value of p_j and the linearly fitted value.

the pictures of deformation of the piston-cylinder under pressure [5]. From the experimental standpoint, one possible way is using the fall- rate data only at higher jacket pressure, where the expansion of the cylinder is prevented by p_j. Another possibility is designing the housing so that the clearance between the piston and cylinder is kept in parallel by the application of jacket pressure. This condition can be implemented by changing the area and position of the cylinder on which p_j is applied.

In this section, we focus on the second possibility, and would like to discuss the effect of the sleeve length in the housing on the deformational characteristics in response of the jacket pressure.

Fig. 6 shows a schematic drawing of the CC piston-cylinder packed in a housing. In the figure, p_j is applied on the area where a sleeve is placed. L is the length of the sleeve. For all kinds of the CC piston-cylinder, L is originally 35 mm; most part of the cylinder is covered with the sleeve and is subjected to the force by p_j. Judging from the results of the characterization experiments, as shown in Fig. 2 and Fig. 3, this length is suitable for the 100 MPa and 200 MPa piston-cylinders. However, from an experimental point of view, it seems too long for piston-cylinders for higher pressure ranges; the application of p_j on the broad

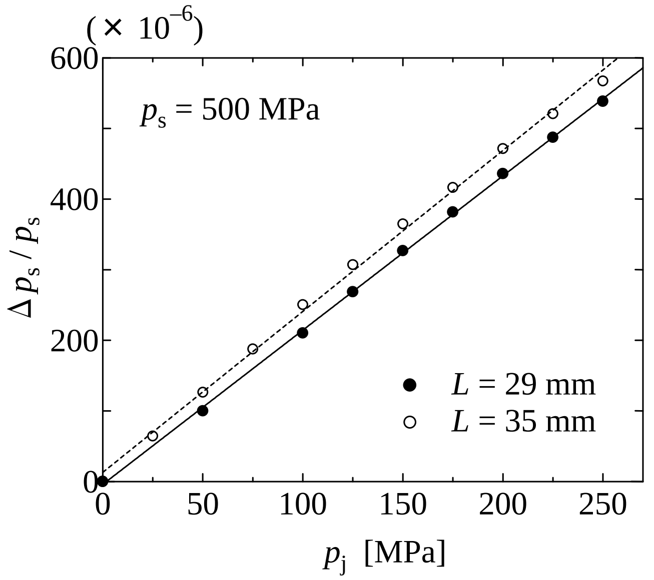

Fig. 8 Relative change in the system pressure, $\Delta p_s/p_s$ against the applied jacket pressure at p_s = 500 MPa for the 500 MPa CC piston-cylinder with different length of the sleeve, L, in the housing; ○ for L = 35 mm and ●for L = 29 mm.

range of the cylinder can cause excessive distortion of the upper part of the cylinder.

To change the area and position on which p_j is applied, the sleeves of different length were prepared and installed in the housing. Then, the effects of the sleeve length on the deformational characteristics were studied. As a trial, the sleeve for a 500 MPa CC piston-cylinder assembly was changed from 35 mm to 29 mm, then, the characterization experiments were performed in a similar way. Fig. 7 shows the effect of the sleeve length on the piston fall-rate. The change in the fall-rate due to the application of p_j is shown in Fig. 7(a), in which p_j is plotted against $v^{1/3}$. The piston fall-rate at p_j = 0 is almost the same, that ensures a good repetition in the installation operations. At other p_j (p_j > 0), the fall-rate in the condition of L = 29 mm is larger than that of L = 35 mm. The lines in the figure are the linearly fitted lines to the data.

To take a closer look at the degree of curvature of the data in Fig. 7(a), the difference of the original value of p_j from the linearly fitted value is plotted in Fig. 7(b). The deviation from the straight line is highly suppressed in the case of L = 29 mm. The change in the sleeve length also affects the standard error of p_z which is obtained as the y-intercept of the fitting line. The resultant p_z in the case of L = 29 mm was 378,3 MPa ± 1,7 MPa, while p_z in the case of L = 35 mm was 350,6 MPa ± 5,4 MPa. The standard error of p_z was largely reduced due to the good linearity of the data.

Fig. 8 shows the relative change in the pressure, $\Delta p_s/p_s$, due to the application of p_j at p_s = 500 MPa. In the case of L = 35 mm, the increasing rate of $\Delta p_s/p_s$ becomes smaller with increasing p_j like the 1 GPa CC piston-cylinder shown in Fig. 5. In the case of L = 29 mm, on the other hand, the relative change in the pressure becomes smaller and the deviation from the linear fit is reduced. The difference of $\Delta p_s/p_s$ between in the case of L = 35 mm and L = 29 mm shows a maximum (approximately 40 $\times 10^{-6}$) at p_j = 100 MPa, and then becomes smaller at lower and higher p_j.

Even if the $\Delta p_s/p_s$ nonlinearly depends on p_j, i.e., d depends on p_j, we can use the results of the cross-float measurements directly in the estimation of effective area by revising the formula (1). When d depends both on p_s and p_j, the forth term of the right-hand side of (1), is revised into more general form as,

$$1+\int_{p_j}^{p_z} d(p_j{}') \; dp_j{}' \; . \tag{4}$$

Once p_z is appropriately estimated, the pressure dependence of the effective area would be precisely estimated with the use of the revised form [4].

From the experimental results shown in Fig. 7 and Fig.8, it was found that the change in the sleeve length can change the jacket pressure dependence of v and $\Delta p_s/p_s$. For the 500 MPa CC piston-cylinder, the housing with the sleeve of 29 mm is showed better linearity in the relationships between the jacket pressure and the cubic root of the piston fall-rate, resulting in the estimation of p_z with smaller error. We are planning to change the length and position of the sleeve precisely to select the best condition.

For other CC piston-cylinders of different pressure ranges, especially for 1 GPa piston-cylinder, it is also expected that the best condition of the sleeve length and position is able to be realized by comparing the deformational characteristics of different sleeve conditions.

6. CONCLUSIONS

A new controlled-clearance pressure balance is originally developed in NMIJ with the aim of improving hydraulic pressure standard in the pressure range up to 1 GPa. We focused on the pressure dependence of the effective area, and performed the characterization experiments based on the Heydemann-Welch model. The results of the several controlled-clearance piston-cylinders are exemplified in this paper. The piston-cylinders for 500 MPa and 1 GPa showed different characteristics at high system pressures from those expected by the H-W model. The area and position of the cylinder on which the jacket pressure is applied was changed by the change in the length of the sleeve in the housing. Then the effects of the sleeve length on the deformational characteristics in response of the jacket pressure were studied. The 500 MPa piston-cylinder with shorter sleeve showed better linearity in the relationships between the jacket pressure and the cubic root of the piston fall-rate, resulting in the estimation of p_z with smaller error. Then, it is expected that the best condition that meets the assumptions of the H-W model can be realized for each CC piston-cylinder by changing the area and position on which the jacket pressure is applied.

REFERENCES

[1] H. Kajikawa, T. Kobata and A. Ooiwa, “Features of a New Controlled-clearance Pressure Balance an *In Situ* Mass

Calibration of Its Weights" *Trans. of the Society of Instrument and Control Engineers*, vol. 44, No. 3, pp. 219 – 226, 2008.

[2] P. L. M. Heydemann and B. E. Welch, *Experimental Thermodynamics*, Vol. II, Chapter 4, Part 3, pp. 147-202, International Union of Pure and Applied Chemistry, London, 1975.

[3] H. Kajikawa, K. Ide and T. Kobata, "Estimation of the Effective Area of the Controlled-Clearance Pressure Balance for Pressures up to 500 MPa" *Proceedings of SICE Annual Conference 2008*, pp. 1544-1547, Tokyo, Japan, Aug. 2008.

[4] H. Kajikawa, K. Ide and T. Kobata, "Precise determination of the jacket pressure coefficient of controlled-clearance pressure balances" *Proceedings of IMEKO 20th TC3，3rd TC16 and 1st TC22 International Conference 2007*, ID-073, Merida, Mexico, Nov. 2007.

[5] G. Buonanno, G. Ficco, G. Giovinco and G. Molinar, *Ten Years of Experience in Modelling Pressure Balances in Liquid Media up to Few GPa*, Universita degli Studi di Cassino, Cassino, 2007.